

## Supporting Information

### Controlled chemical assembly of enzyme in cell lysate enabled by genetic-encoded nonstandard amino acid

Jing Zhang, Ru Wang, Zhiyuan Luo, Dongmei Jia, Haomin Chen, Qinjie Xiao, Pengfei Zhang, \* Xiaolin Pei and Anming Wang\*

---

J. Zhang, Z. Luo, H. Chen, Q. Xiao, Prof. X. Pei, Prrof. P. Zhang, Prof. A. Wang

College of Material, Chemistry and Chemical Engineering, Key Laboratory of

Organosilicon Chemistry and Material Technology, Ministry of Education

Hangzhou Normal University

No. 2318, Road Yuhangtang, Hangzhou, Zhejiang 311121, China

E-mail: [zpf@hznu.edu.cn](mailto:zpf@hznu.edu.cn); [waming@hznu.edu.cn](mailto:waming@hznu.edu.cn)

R. Wang, School of Pharmacy, Key Laboratory of Elemene Class Anti-Cancer

Chinese Medicines; Engineering Laboratory of Development and Application of

Traditional Chinese Medicines; Hangzhou Normal University,

No. 2318, Road Yuhangtang, Hangzhou, Zhejiang 311121, China

**30 September 2022**

**Note added after first publication:** This supplementary information file replaces that originally published on 30 November 2021. The compound (R)-3,5-bis (trifluoromethyl) phenylethanol was incorrectly shown in the S-conformation in Fig. S6 and S8-11 in the original version. This has been corrected in this updated version.

## 1. Materials and methods

### 1.1 Materials

Both *E. coli* DH5 $\alpha$  bacteria and *E. coli* BL21(DE3) used in the study were obtained from Stratagene and Novagen. The endonucleases and primers used in this study were bought and synthesized by Shanghai Jerry Biotechnology Co. Ltd. (Shanghai). Antibiotics such as chloramphenicol, kanamycin, and ampicillin were all purchased from Biotech. (Shanghai). The non-standard amino acid *p*-Azido-L-phenylalanine (p-AzF) was purchased from Artis Biotechnology Co. Ltd. The inducer anhydrous tetracycline hydrochloride (aTc) and dihydro-4,4-dimethyl-2,3-furandione (ketone lactone) were obtained from Sigma-Aldrich. Unless otherwise specified, NADPH was purchased from J&K Scientific Ltd. *sym*-Dibenzo-1,5-cyclooctadiene-3,7-diyne (diyne), other chemical reagents were purchased from Sinopharm Chemical Reagent (Shanghai) Co. Ltd. and other biological reagents purchased from Biotech. In the site-directed mutagenesis, PCR method was used to mutate the genes of target sites. Genomically recoded organism (GRO) C321. $\delta$ A (MG1655) was used to express NSAAs modified enzymes to increase protein expression. In our experiment, all solutions were prepared with deionized water as the medium. The resistance(s) of the plasmid to ampicillin (MG1655), chloramphenicol (pEVOL-pAzF) and kanamycin (pZE21-GFPaav) were 50 $\mu$ g·mL and 34 $\mu$ g·mL, respectively.

### 1.2 Plasmid Construction, Protein Expression, and Characterization.

#### 1.2.1 Site Pre-selection

We selected 5 different two-point sites (114Y-189Y), (3Y-31Y), (3Y-189Q), (3Y-232W) and (198Y-232W) according to AKR structure, and named them AKR two-point mutants. Plasmid pZE21-GFPaav<sup>1</sup> obtained from Addgen was used as the target vector to produce aldehyde keto reductase (AKR, PDB ID: 5dan.1; resolution: 2.0 Å) from *Thermotoga maritima* MSB8 in GRO MG1655. For produce some free enzyme for control, a C-terminal His 6 tag was also encoded. A site-directed mutagenesis PCR method was used to introduce an amber codon (UAG) at position 114 (Y) to replace the tyrosine codon. Multi-point mutant genes are subjected to multiple site-

directed mutations based on single-point mutations. We selected multiple mutation sites which are far from AKR active site, including pZE21-AKR 3(Y), 31(Y), 114(Y), 189(Q), 198(Y) and 232(W) <sup>2</sup>. Site-directed mutagenesis primers such as Table S1 shows. The plasmid pEVOL-pAzF (tRNA synthase /tRNA pair) is used to insert pAzF in vivo into proteins that respond to the amber codon TAG, from Peter G. Schultz's group at the Scripps Research Institute <sup>3</sup>. MG1655 was co-transformed by pAzF and pEVOL-pAzF, and pAzF was mixed into the mixture <sup>4</sup>.

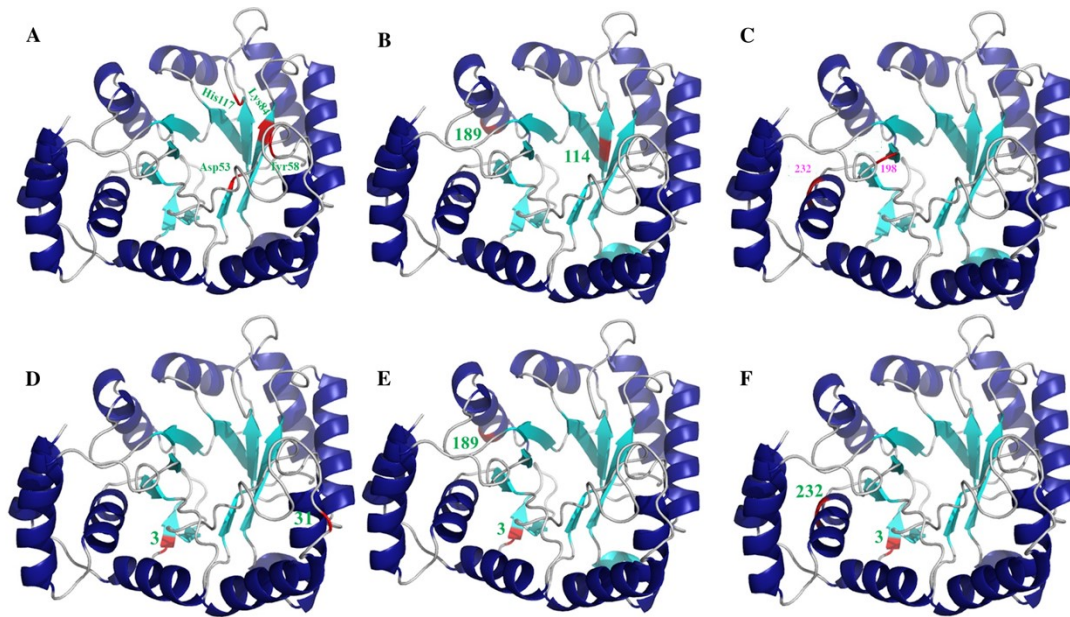


**Figure S1 Three-dimensional map of the loci of the AKR two-point mutant**

### 1.2.2 *akr* Gene for encoding AKR enzyme

```

ATGCTGTACAAAGAACTGGGCCGTACCGGTGAAGAAATTCGGCCTTAGG
CTTAGGCACCTGGGGTATTGGCGGCTTTGAAACCCCGGATTATTCTCGCGA
TGAAGAAATGGTGGAACTGTTAAAACCGCAATTAATAATGGGCTATACCC
ATATTGATACCGCAGAATATTATGGCGGCGGTCATACCGAAGAACTGATT
GGTAAAGCCATTAAAGATTTTCGTCGCGAGGATCTGTTTATTGTGTCTAAA
GTGTGGCCGACCCATCTGCGCCGTGATGATCTGCTGCGCTCTCTGGAAAAT
ACCCTGAAACGTTTAGATACCGATTATGTGGATCTGTATCTGATTCATTGG
CCGAATCCGGAAATTCGCTGGAAGAAACCCTGAGTGCAATGGCAGAAG
GCGTGCGTCAGGGCTTAATTCGCTATATTGGTGTGAGTAATTTTGATCGTC
GCCTGCTGGAAGAAGCCATTTCTAAATCACAGGAACCGATTGTTTGTGAT

```

CAGGTTAAATATAATATTGAAGATCGCGATCCGGAACGCGATGGTTTACT  
GGAATTTTGTGAGAAAAATGGCGTGACCTTAGTTGCCTATAGTCCGTTACG  
TCGTACCTTACTGAGTGAAAAACCAAACGCACCTTAGAAGAAATTGCCA  
AAAATCATGGTGCCACCATATACCAGATTATGTTAGCATGGCTGTTAGCC  
AAACCGAATGTGGTTGCAATTCCGAAAGCAGGTCGTGTTGAACATCTGCG  
CGAAAATCTGAAAGCAACCGAAATTAACTGAGCGAAGAAGAGATGAAA  
CTGCTGGATAGTCTGGGTAA

### 1.2.3 *AKR sites-specific mutation*

**Table S1 Primers for AKR sites mutations**

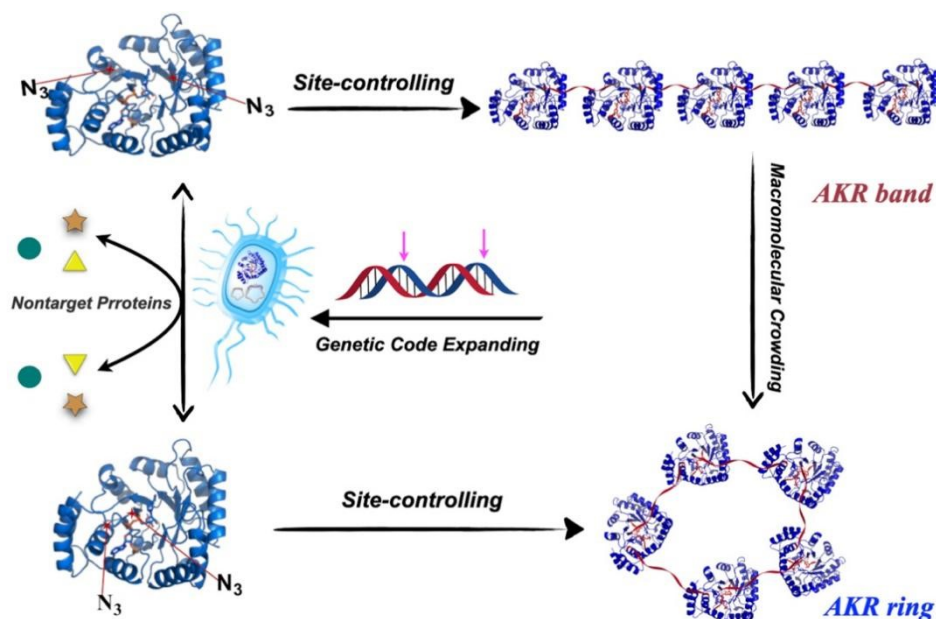
Primer	Sequence (5'→3')	T <sub>m</sub> (°C)
AKR3Y-F	aaaggtaccatgctgtagaaagaactgggcccgt	60
AKR3Y-R	acggcccagttctttctacagcatggtacctt	60
AKR-31Y-F	ttagaaaccccgattagctctcgcatgaagaa	58
AKR-31Y-R	ttcttcacgcgagactaatccggggttcaaa	58
AKR-232W-F	cagattatgtagcatagctgtagccaaaccg	62
AKR-232W-R	cggtttgctaacagctatgctaataatctg	61
AKR-198Y-F	gtgaccttagttgcctagagtcggttacgtct	59
AKR-198Y-R	acgacgtaacggactctaggcaactaaggtcac	59
AKR-114Y-F	GATTATGTGGATCTGT <u>AG</u> CTGATTCATTGGCCG	60
AKR-114Y- R	CGGCCAATGAATCAGCT <u>A</u> CAGATCCACATAAT C	59
AKR-189Q-F	TTACTGGAATTTTGT <u>TA</u> GAAAAATGGCGTGACC	59
AKR-189Q-R	GGTCACGCCATTTT <u>CTA</u> ACAAAATTCCAGTAA	58

The experimental methods for the expression and purification of specific proteins are derived from our previous work <sup>5, 6</sup>. Plasmids containing the AKR multipoint mutation gene were grown overnight in LB, oscillated at 34°C, and the appropriate antibiotics were added to LB. The medium was diluted 100 times and re-amplified in fresh LB containing antibiotics to enlarge the plasmid culture. These cultures were

cultured to  $OD_{600}$  of 0.5, and 0.2% L-arabinose was added to induce pEVOL-pAzF for 1h. To culture to an  $OD_{600}$  of 0.6, we added  $30 \text{ ng}\cdot\text{mL}^{-1}$  aTc and 1mM pAzF. The protein was expressed by continuous shaking at 23 °C for 16 h. The induced enzymes were treated with ultrasonic disruption and purified by Ni column. We use SDS-PAGE to examine the protein expression and matrix-assisted laser desorption/ionization time-of-flight mass spectrometry (MALDI-TOF MS; Bruker Ultraflextreme) to verify the actual relative molecular mass of the obtained target protein.

After expressing the enzyme protein for 16 h, the cultured cells were harvested, re-suspended in PBS buffer (20 mM, pH 7.0) and lysed by ultrasound. The AKR two-point mutant protein was further purified by using Ni-NTA agarose (Ni Sepharose 6 Fast Flow). To test whether the pAzF NSAA was inserted into the fixed sites of the AKR peptide chain as expected, we used matrix assisted laser desorption/ionization time of flight mass spectrometry (MALDI-TOF MS) and Microflex MALDI-TOF mass spectrometry to analyze the exact molecular mass. We used methanol as the substrate and solvent to dissolve protein samples during TOF analysis. The protein solution sample was then applied to a clean target board, air-dried at room temperature, and the obtained data was analyzed using a Microflex system.

### 1.3 Preparation and Characterization of the covalent assembly of AKR mutants using cell lysate



**Scheme 1 Schematic process of preparing and assembling the two-point AKR mutants**

#### 1.3.1 Assembly of the AKR two-point mutants

In a preliminary study, diyne was dissolved in isopropanol ( $0.66 \text{ mg}\cdot\text{mL}^{-1}$ ), and the solution was added to 1 mL  $0.1 \text{ mol}\cdot\text{L}^{-1}$  PBS, pH 7.0, containing the two-point mutant. The molar ratio of azide to alkyne group in the reaction is 1:1/1:2. The mixture inside the container is placed in a microwave reactor equipped with a cooling module and irradiated for a period of time (Discover CoolMate, CEM, USA). The temperature gap between the microwave reactor and the cooling module is controlled by continuous illumination.

In order to verify the covalently cross-linked AKR multipoint mutants under continuous microwave irradiation, the cross-linked enzymatic hydrolysis was performed using  $6 \text{ mol}\cdot\text{L}^{-1}$  hydrochloric acid at  $110 \text{ }^\circ\text{C}$  for 24 h. The sample was hydrolyzed and washed with deionized water for four times. Methanol was used as the solvent for analytical mass spectrometry.

#### 1.3.2 Characterization of the obtained assembly of AKR mutants

##### Scanning Electron microscopy characterization

The assembly and shape of the two-point mutants at different sites were

characterized by scanning electron microscopy (JEOL-5600LV). The protein samples were cross-linked and assembled under microwave radiation, and the precipitates were obtained by centrifugation. After taking 100  $\mu$ L of anhydrous ethanol to re-suspend the protein samples, 10  $\mu$ L of the sample solution was taken as a drop on tin foil and air-dried. All microscopic images were obtained under a scanning electron microscope at 3.0 kV.

#### *Transmission Electron Microscope characterization*

When characterizing the obtained assembly using transmission electron microscope (TEM), samples were diluted to final concentrations between 0.5 and 2 nM and adsorbed on glow discharged Formvar-supported carbon-coated Cu400 TEM grids (Science Services, Munich). TEM measurements were performed on a JEOL model JEM-3010 at 300 kV.

#### *Atomic force microscopy characterization*

Atomic force microscopy (AFM) was used to obtain topographic maps of AKR-CLEs using a silicon tip (Nano sensors, Switzerland) with a spring constant of 1.4 N/m, in the knockdown mode of E-Sweep (Seiko Instruments, Japan). The same. The obtained protein samples were dissolved in 100  $\mu$ L of anhydrous ethanol, and 10  $\mu$ L of the samples were deposited on freshly cleaved silicon wafers and air-dried. The silicon wafer was then placed on a holder on top of the scanning tube for AFM observation. Sample height and phase images were recorded and analyzed using the Nano scope software provided by the AFM manufacturer.

#### *CLSM characterization*

The assembled morphology of AKR two-site enzyme aggregates was examined by confocal laser scanning microscopy (CLSM). The obtained AKR two-site enzyme aggregates were stained with fluorescent isothiocyanate (FITC) for 12 h at 4°C, with 0.01 mg of fluorescein corresponding to each 1 mg of protein. After staining, the samples were washed more than 3 times with pH 8.0 buffer solution, and finally a small amount of sample was dropped onto the slide and air-dried, covered with a coverslip. The morphology of protein aggregates was observed under CLSM, and then the samples were analyzed using a laser scanning confocal microscope (Olympus

FV 1000 CLSM). Under 405 nm excitation, the enzyme protein obtained green fluorescence in the range of 480 ~ 540 nm.

#### *Dynamic light and static light scattering*

Static light scattering (SLS) and dynamic light scattering (DLS) were used to characterize the size of the cyclic protease assembly. All samples for light scattering experiments were prepared by methods designed to maximally reduce dust contamination. The protein assembly was re-suspended with 0.02 M pH 7.0 PBS buffer at a concentration of  $1.5\text{mg}\cdot\text{mL}^{-1}$  and used for dynamic light scattering experiments. For static light-scattering (SLS) experiments, six samples were prepared, extending from 5 to 40 mM (0.17-1.41 mg/mL) total protein concentration <sup>7</sup>. Light scattering data were obtained at the wide-angle dynamic (static) light scattering instrument (BI-200SM/ Nanobrook Zetapals /BI-DNDC) at Westlake University.

#### *1.3.3 Examination of the covalent assembly of AKR mutants*

##### *FT-IR spectra*

After microwave treatment, the enzyme-protein combination was air-dried to remove surface water and the purified free enzyme was freeze-dried. The ground dried KBr was mixed and ground with the enzyme-protein sample in a ratio of 100:1 and a small amount was taken for compression. Their structures were determined by Fourier transform infrared spectroscopy. Then, a Gaussian fit was performed with Peakfit to fit the IR data analytically.

##### *Mass spectrometry analysis*

To validate the covalent cross-linking of AKR multipoint mutants under continuous microwave radiation, the cross-linked enzyme was hydrolyzed using  $6\text{mol}\cdot\text{L}^{-1}$  hydrochloric acid at 110 °C for 24 h. The hydrolyzed samples were then washed four times with deionized water and analyzed by mass spectrometry using acetonitrile as solvent and the samples were filtered using 0.22  $\mu\text{m}$  organic filter tip. The molecular weights of the fractions were detected and analyzed by MS in acetonitrile solvent.



## **1.4 Stability of the AKR assembly against heating treatment and digestion by gastric juice and intestinal fluids**

### *1.4.1 Thermal stability*

In order to evaluate the thermal stability of AKR assembly, the fast and accurate cross-linking enzyme was transferred to the reaction medium and incubated at 30, 40, 50, and 60°C in a water bath for the same times. Then, periodically extract samples from the suspension and determine the activity of the fragments as the previous report<sup>8</sup>. The initial activity is set to 100%, and the thermal stability is the remaining activity (% basis)<sup>9, 10</sup>, which is the ratio of the remaining activity after AKR assembly heating to the initial activity.

### *1.4.2 Stability against the digestion using gastric juice and intestinal fluids*

In order to study the effects of gastric and intestinal fluids on the stability of AKR assembly. Simulated gastric juice (SGJ)<sup>11, 12</sup> was composed of 2.0 g NaCl and 32mg pepsin (3000:1), and hydrochloric acid solution with pH 1.5 was added to the volume to 10mL. Simulated intestinal fluid (SIF): take KH<sub>2</sub>PO<sub>4</sub> 46.8g and add 500mL water to dissolve, adjust pH to 6.5 with 0.4% (w/w) NaOH. Add 1g trypsin per 100mL of liquid and mix well. AKR assembly were added into the prepared simulated gastric juice and simulated intestinal juice, respectively, and the ratio of enzyme to simulated environment liquid was 1:4 (V/V). The sample was placed in a shaker at 37 °C and 50 rpm for 2 h, and the enzyme activity was measured by sampling every half an hour.

## **1.5 Enzymatic synthesis of (R)-1-[3',5'-bis(trifluoromethyl)phenyl] ethanol using AKR assembly**

Enzyme aggregates are used to catalyze the synthesis of 3,5-bis(trifluoromethyl) phenylethanol. The 5 mL solution consisted of 100 mM PBS buffer (pH=7.0), 27mg NADP<sup>+</sup>, 3mg substrate, 1 mM [CP\*RH (BPY) (H<sub>2</sub>O)]<sup>2+</sup>, 4 mg TiO<sub>2</sub> nanotubes, and 2 mg enzyme aggregates. The solution was placed in a quartz reactor with a small agitator and illuminated by a xenon lamp with a wavelength of 420 nm (500 W, DY500G)<sup>13, 14</sup>. To avoid increasing the temperature of the reaction mixture, the

xenon lamp is placed approximately 15 cm from the reactor. The product in the reaction supernatant was extracted with 20 ml of anhydrous heptane and analyzed by high performance liquid chromatography. In content analysis, the ratio of isomers can be determined by high performance liquid chromatography (HPLC, Agilent 1260). The final product was separated by liquid chromatography on a Daicel IC column (210 mm 4.6 mm, particle size 5  $\mu$ m). The pump runs at a flow rate of 0.5 mL $\cdot$ min<sup>-1</sup>. Solvent A is water; solvent B is methanol. The volume ratio of water to methanol is 25:75 (v/v). The temperature of the auto sampler is kept at 20°C, and the injection volume is 10  $\mu$ L each time. The data was collected at 210 nm, and the corresponding standards were used to verify the retention time of the substrate and target product standards.

## 2. Results

### 2.1 SDS-PAGE

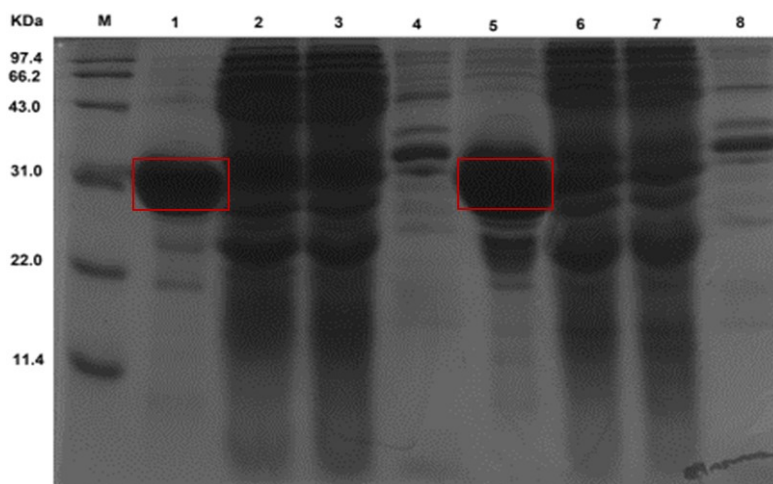


**Figure S2** SDS-PAGE analysis of AKR-3Y-31Y and AKR-3Y-189Q produced in the presence of pAzF. Lane M, protein marker; lane 1, Purified AKR-3Y-31Y; lane 2, culture supernatant of AKR-3Y-31Y; lane 3, cellular soluble fraction of AKR-3Y-31Y; lane 4, cellular insoluble fraction of AKR-3Y-31Y; lane 5, Purified AKR-3Y-189Q; lane 6, culture supernatant of AKR-3Y-189Q; lane 7, cellular soluble fraction of AKR-3Y-189Q; lane 8, cellular insoluble fraction of AKR-3Y-189Q.

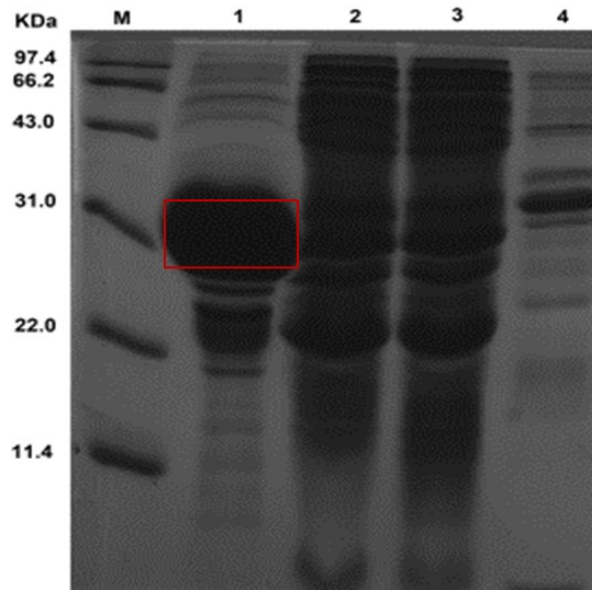


**Figure S3** SDS-PAGE analysis of AKR-3Y-232W produced in the presence of pAzF. Lane M, protein marker; lane 1, Purified AKR-3Y-232W; lane 2, culture supernatant of AKR-3Y-232; lane 3, cellular soluble fraction of AKR-3Y-232; lane 4, cellular insoluble fraction of AKR-3Y-232W.

### 3.2 AFM

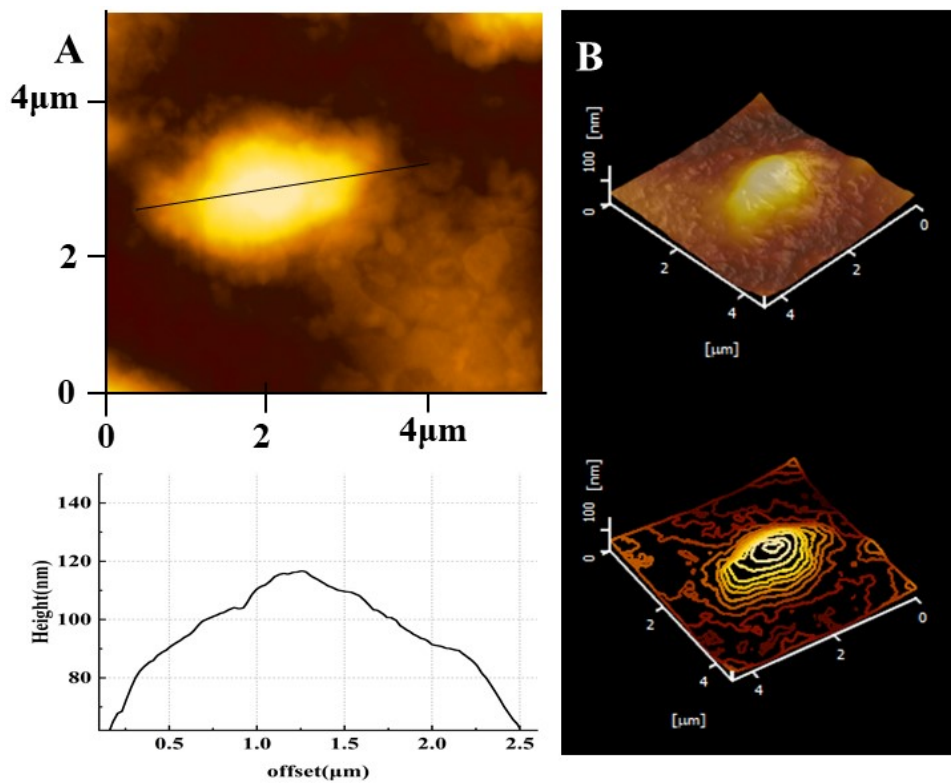


**Figure S4.** Structural analysis by AFM of Cyclic-AKR-CLEs (AKR-198Y-232W, 3min, 10°C and 10W; A, analysis of the morphology and height of Cyclic-AKR-CLEs; B, three-dimensional AFM topography image of an individual structure.)

## 2.3 DLS/SLS

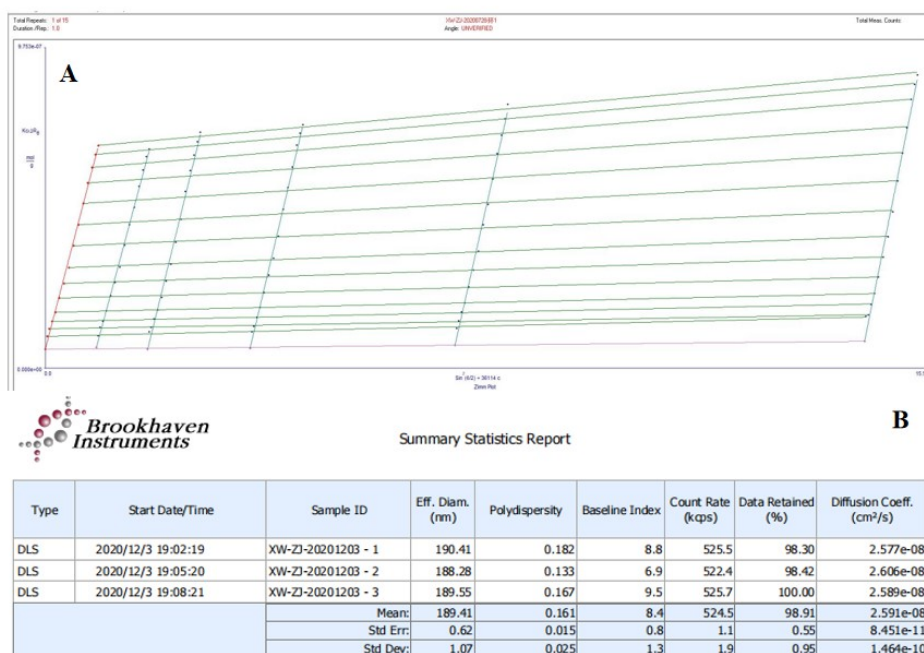


**Figure S5** Static light scattering (SLS, A) and dynamic light scattering (DLS, B) characterization of Cyclic-AKR-198Y-232W. The AKR mutant protein assembly was re-suspended with 0.02 M pH 7.0 PBS buffer at a concentration of 1.5mg·mL<sup>-1</sup> and used for dynamic light scattering experiments; For static light-scattering experiments, six samples were prepared, extending from 5 to 40 mM (0.17-1.41 mg·mL<sup>-1</sup>) total protein concentration.

## 2.4 HPLC

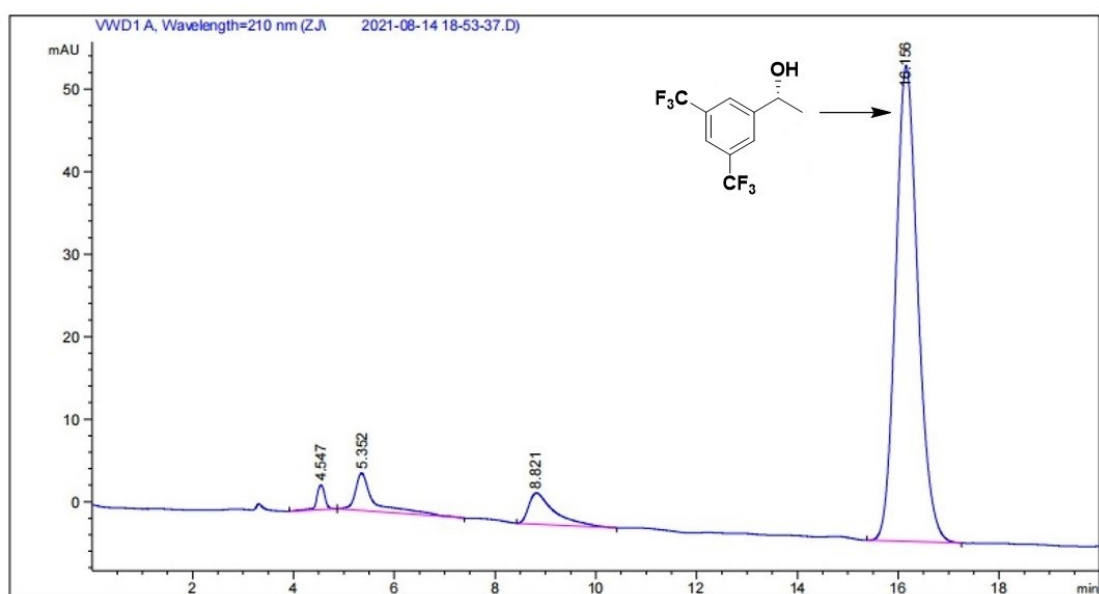


**Figure S6** Reversed-phase HPLC of (R)-1-[3',5'-bis(trifluoromethyl)phenyl] ethanol. The pump runs at a flow rate of  $0.5 \text{ mL} \cdot \text{min}^{-1}$ ; Solvent A is water; solvent B is methanol; The volume ratio of water to methanol is 25:75 (V/V); The data was collected at 210 nm and the injection volume is  $10 \mu\text{L}$  each time.

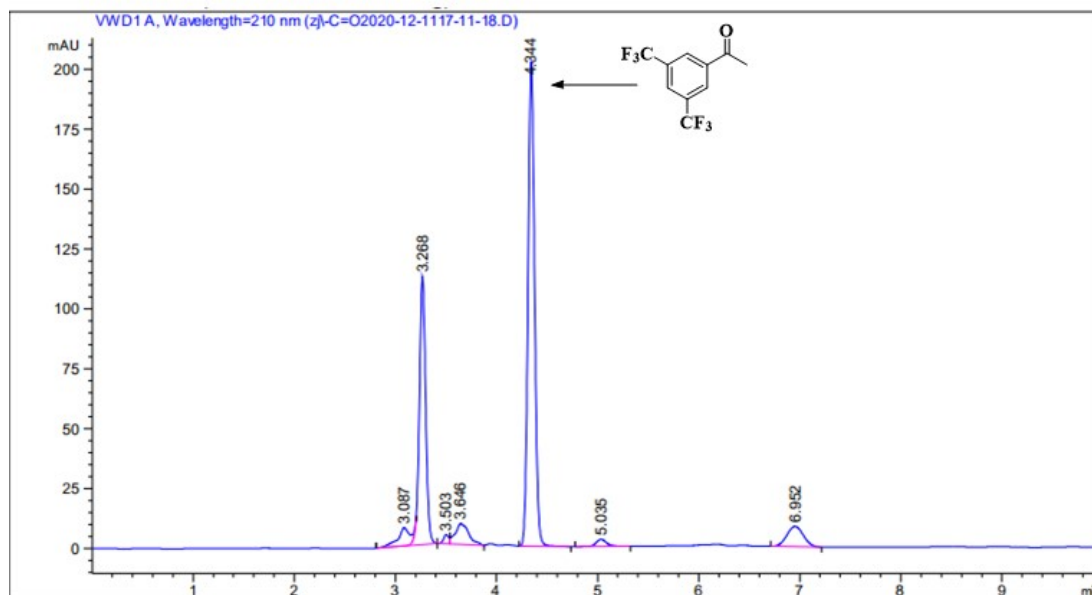


**Figure S7.** Normal phase HPLC of 3,5-bis(trifluoromethyl) acetophenone. The pump runs at a flow rate of  $1 \text{ mL} \cdot \text{min}^{-1}$ ; Solvent A is n-hexane; solvent B is isopropanol; The volume ratio of n-hexane to isopropanol is 2:98 (v/v); The data was collected at 210 nm and the injection volume is  $10 \mu\text{L}$  each time.

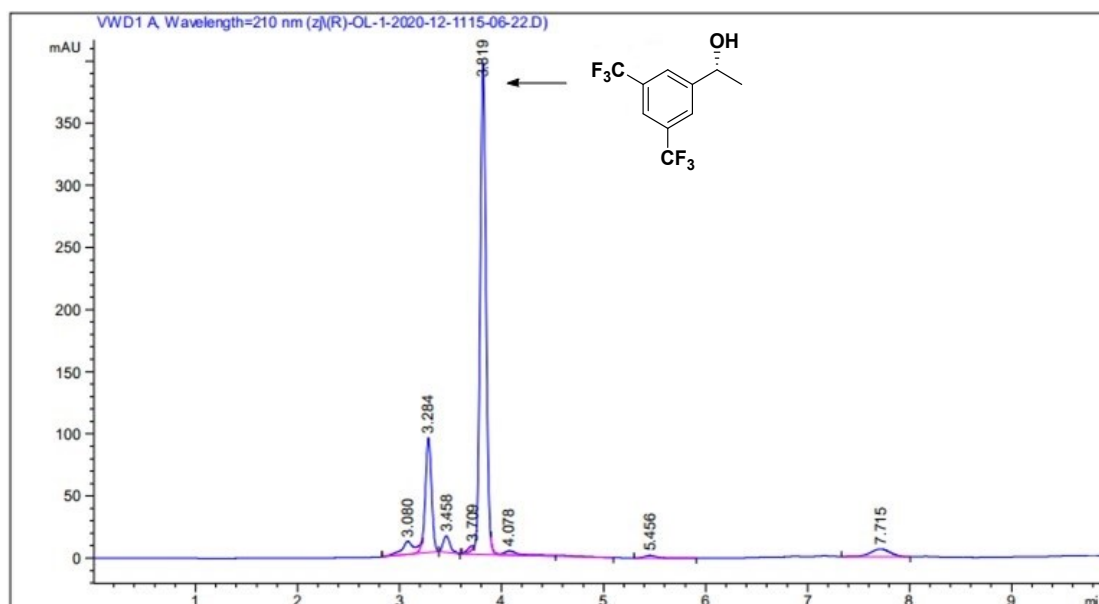


**Figure S8** Normal phase HPLC of (R)-1-[3',5'-bis(trifluoromethyl)phenyl] ethanol. The pump runs at a flow rate of  $1 \text{ mL} \cdot \text{min}^{-1}$ ; Solvent A is n-hexane; solvent B is isopropanol; The volume ratio of n-hexane to isopropanol is 2:98 (v/v); The data was collected at 210 nm and the injection

volume is 10  $\mu\text{L}$  each time.

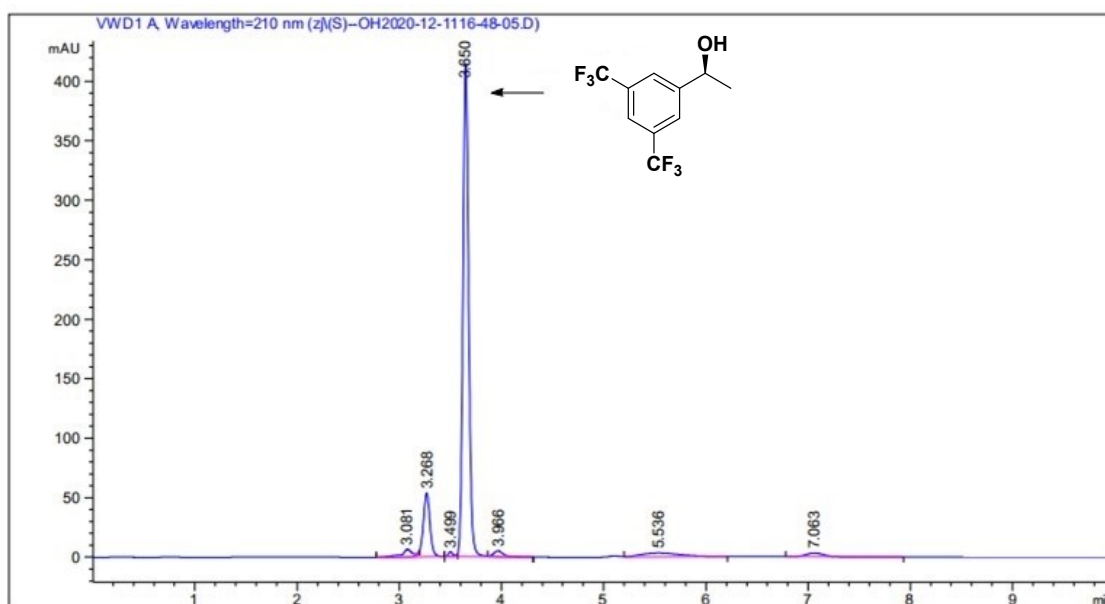


**Figure S9** Normal phase HPLC of (S)-1-[3',5'-bis(trifluoromethyl)phenyl] ethanol. The pump runs at a flow rate of 1  $\text{mL}\cdot\text{min}^{-1}$ ; Solvent A is n-hexane; solvent B is isopropanol; The volume ratio of n-hexane to isopropanol is 2:98 (v/v); The data was collected at 210 nm and the injection volume is 10  $\mu\text{L}$  each time.

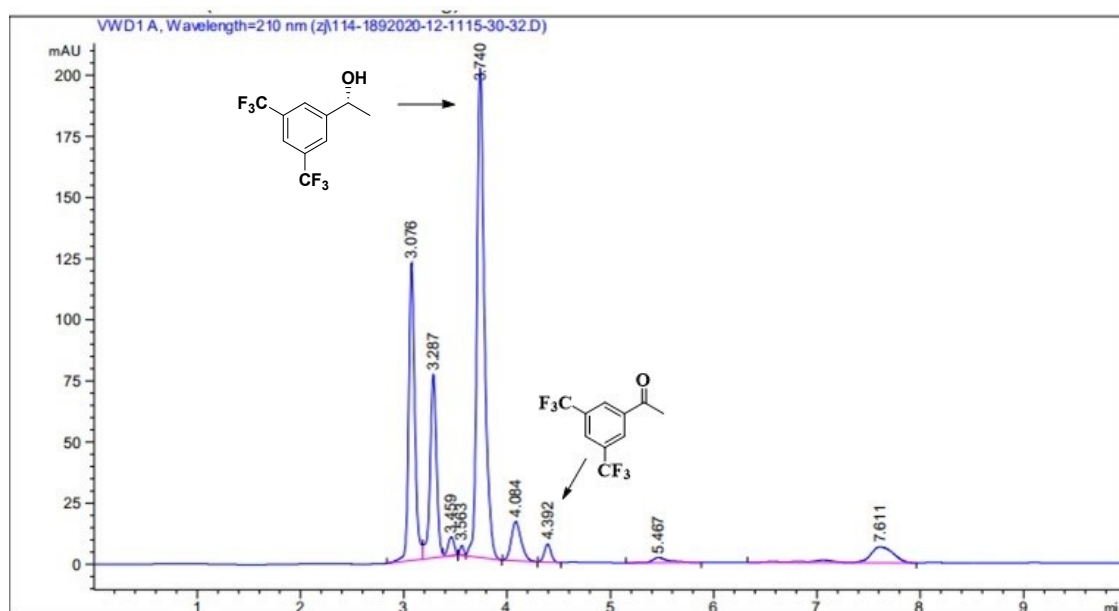


**Figure S10** Normal phase HPLC analysis of the synthesized (R)-1-[3',5'-bis(trifluoromethyl)phenyl] ethanol using Banded-AKR-CLEs (t=16 h).

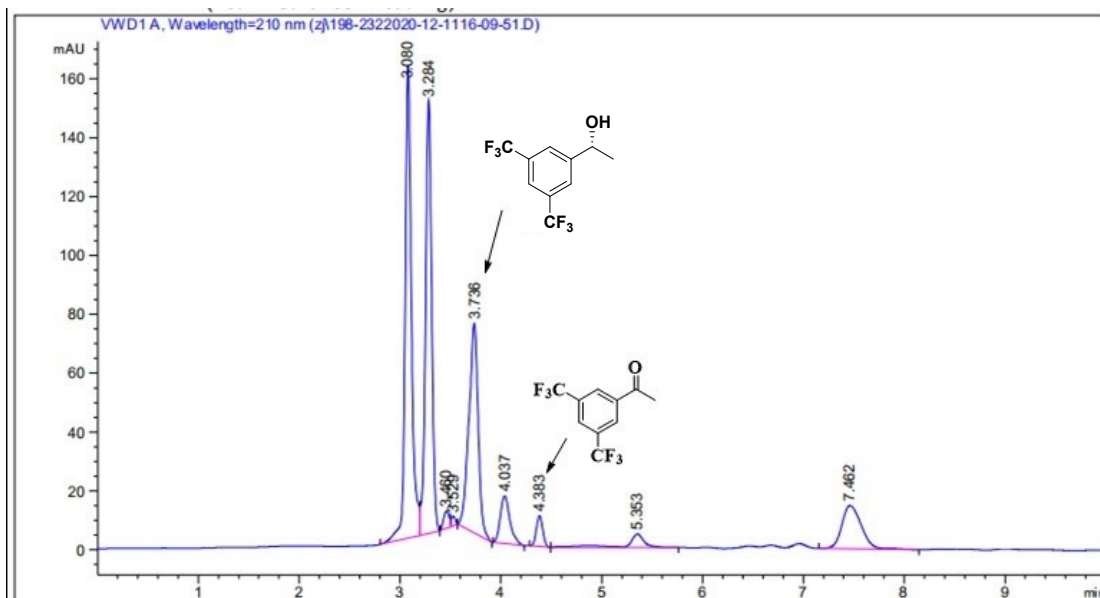


**Figure S11** Normal phase HPLC analysis of the synthesized (R)-1- [3',5'-bis (trifluoromethyl) phenyl] ethanol using Cyclic-AKR-CLEs (t=16 h).

## References

1. M. B. Elowitz and S. Leibler, A synthetic oscillatory network of transcriptional regulators, *Nature*, 2000, **403**, 335-338.
2. C. Zhang, Z. Min, X. Liu, C. Wang, Z. Wang, J. Shen, W. Tang, X. Zhang, D. Liu and X. Xu, Tolrestat acts atypically as a competitive inhibitor of the thermostable aldo-keto reductase Tm1743 from *Thermotoga maritima*, *FEBS Lett.*, 2020, **594**, 564-580.
3. J. W. Chin, S. W. Santoro, A. B. Martin, D. S. King, L. Wang and P. G. Schultz, Addition of p-Azido-l-phenylalanine to the Genetic Code of *Escherichia coli*, *J. Am. Chem. Soc.*, 2002, **124**, 9026-9027.
4. M. J. Lajoie, A. J. Rovner, D. B. Goodman, H.-R. Aerni, A. D. Haimovich, G. Kuznetsov, J. A. Mercer, H. H. Wang, P. A. Carr, J. A. Mosberg, N. Rohland, P. G. Schultz, J. M. Jacobson, J. Rinehart, G. M. Church and F. J. Isaacs, Genomically Recoded Organisms Expand Biological Functions, *Science*, 2013, **342**, 357-360.
5. H. Li, Y. Yin, A. Wang, N. Li, R. Wang, J. Zhang, X. Chen, X. Pei and T. Xie, Stable immobilization of aldehyde ketone reductase mutants containing nonstandard amino acids on an epoxy resin via strain-promoted alkyne-azide cycloaddition, *Rsc Advances*, 2020, **10**, 2624-2633.
6. H. Li, R. Wang, A. Wang, J. Zhang, Y. Yin, X. Pei and P. Zhang, Rapidly and Precisely Cross-Linked Enzymes Using Bio-Orthogonal Chemistry from Cell Lysate for the Synthesis of (S)-1-(2,6-Dichloro-3-fluorophenyl) Ethanol, *Acs Sustainable Chemistry & Engineering*, 2020, **8**, 6466-6478.
7. J. C. T. Carlson, S. S. Jena, M. Flenniken, T.-f. Chou, R. A. Siegel and C. R. Wagner, Chemically controlled self-assembly of protein nanorings, *Journal of the American Chemical Society*, 2006, **128**, 7630-7638.
8. Z. Magomedova, A. Grecu, C. W. Sensen, H. Schwab and P. Heidinger, Characterization of two novel alcohol short-chain dehydrogenases/reductases from *Ralstonia eutropha* H16 capable of

- stereoselective conversion of bulky substrates, *Journal of Biotechnology*, 2016, **221**, 78-90.
9. A. Wang, M. Wang, Q. Wang, F. Chen, F. Zhang, H. Li, Z. Zeng and T. Xie, Stable and efficient immobilization technique of aldolase under consecutive microwave irradiation at low temperature, *Bioresour. Technol.*, 2011, **102**, 469-474.
  10. D. Hormigo, J. Garcia-Hidalgo, C. Acebal, I. de la Mata and M. Arroyo, Preparation and characterization of cross-linked enzyme aggregates (CLEAs) of recombinant poly-3-hydroxybutyrate depolymerase from *Streptomyces exfoliatus*, *Bioresour. Technol.*, 2012, **115**, 177-182.
  11. E. Malinauskyte, J. Ramanauskaite, D. Leskauskaite, T. G. Devold, R. B. Schuller and G. E. Vegarud, Effect of human and simulated gastric juices on the digestion of whey proteins and carboxymethylcellulose-stabilised O/W emulsions, *Food Chemistry*, 2014, **165**, 104-112.
  12. F. Tamjidi, M. Shahedi, J. Varshosaz and A. Nasirpour, Stability of astaxanthin-loaded nanostructured lipid carriers as affected by pH, ionic strength, heat treatment, simulated gastric juice and freeze-thawing, *Journal of Food Science and Technology-Mysore*, 2017, **54**, 3132-3141.
  13. K. Lee, A. Mazare and P. Schmuki, One-Dimensional Titanium Dioxide Nanomaterials: Nanotubes, *Chemical Reviews*, 2014, **114**, 9385-9454.
  14. Y. Tachibana, L. Vayssieres and J. R. Durrant, Artificial photosynthesis for solar water-splitting, *Nature Photonics*, 2012, **6**, 511-518.